Shear waves elastography for assessment of human Achilles tendon's biomechanical properties: an experimental study

Thomas-Xavier Haen, Anthony Roux, M. Soubeyrand, Sébastien Laporte

Shear waves elastography for assessment of human Achilles tendon's biomechanical properties: an experimental study

T.X. Haen[a,b,*], A. Roux[a], M. Soubeyrand[c], S. Laporte[a]

[a] *Arts et Metiers ParisTech, Institut de Biomécanique Humaine Georges Charpak, 151 bd de l'Hôpital, 75013 Paris, France*
[b] *Service de Chirurgie Orthopédique, Hôpital Raymond Poincaré (A.P.-H.P), 104 bd Raymond Poincaré, 92380 Garches (Paris area), France*
[c] *Service de Chirurgie Orthopédique, Hôpital de Bicêtre (A.P.-H.P.), 78 rue du Général Leclerc, 94270 Le Kremlin-Bicêtre (Paris area), France*

ARTICLE INFO

Keywords:
Shear waves elastography
Achilles tendon
Cadaveric tendon
Material testing machine

ABSTRACT

Introduction: Achilles tendon is the most frequently ruptured tendon, but its optimal treatment is increasingly controversial. The mechanical properties of the healing tendon should be studied further. Shear waves elastography (SWE) measures the shear modulus, which is proven to be correlated to elastic modulus in animal tendons. The aim of our study was to study whether the shear moduli of human cadaveric Achilles tendon, given by SWE, were correlated with the apparent elastic moduli of those tendons given by tensile tests.

Materials and methods: Fourteen cadaveric lower-limbs were studied. An elastographic study of the Achilles tendon (AT) was first done in clinical-like conditions. SWE was performed at three successive levels (0, 3 and 6 cm from tendon insertion) with elastographic probe oriented parallel to tendon fibers, blindly, for three standardized ankle positions (25° plantar flexion, neutral position, and maximal dorsal flexion). The mean shear moduli were collected through blind offline data-analysis.

Then, AT with triceps were harvested. They were subjected to tensile tests. A continuous SWE of the Achilles tendon was performed simultaneously.

The apparent elastic modulus was obtained from the experimental stress-strain curve, and correlation with shear modulus (given by SWE) was studied.

Results: Average shear moduli of harvested AT, given by SWE made an instant before the tensile tests, were significantly correlated with shear moduli of the same AT made at the same level, previously in clinical-like condition ($p < 0.05$), only in neutral position.

There was a statistical correlation ($p < 0.005$) and a correlation coefficient R^2 equal to 0.95 ± 0.05, between shear moduli (SWE) and apparent elastic moduli (tensile tests), for 11 tendons (3 tendons were inoperable due to technical error), before a constant disruption in the correlation curves.

Discussion: We demonstrated a significant correlation between SWE of Achilles tendon performed in clinical-like conditions (in neutral position) and SWE performed in harvested tendon. We also found a correlation between SWE performed on harvested tendon and apparent elastic moduli obtained with tensile tests (for 11 specimens). As a consequence, we can suppose that SWE of AT in clinical-like conditions is related to tensile tests. To our knowledge, the ability of SWE to reliably assess biomechanical properties of a tendon or muscle was, so far, only demonstrated in animal models.

Conclusion: SWE can provide biomechanical information of the human AT non-invasively.

1. Introduction

Achilles Tendon (AT), which links the triceps surae to the calcaneus, allows the plantar flexion of the ankle. It is one of the most frequently ruptured tendons (Józsa et al., 1989), with increasing incidence (Hess, 2010; Lantto et al., 2014). However the management of AT rupture is still controversial (Bruns et al., 2014; Lantto et al., 2014): in comparison to cast immobilization, surgery helps to prevent re-ruptures, but is associated with more complications, especially infections (Bruns et al., 2014; Lantto et al., 2014). This controversy is due to the fact that little is known about biomechanical properties of the healing tendon (Bruns et al., 2014), especially while comparing different treatments. The only biomechanical studies are animal studies, reporting tensile tests done after animal sacrifice (Marcos

Abbreviations: AT, Achilles Tendon; SWE, Shear Wave Elastography; CSA, Cross-sectional area; ROI, region of interest

* Corresponding author at: Arts et Metiers ParisTech, Institut de Biomécanique Humaine Georges Charpak, 151 bd de l'Hôpital, 75013 Paris, France.
E-mail address: tx.haen@aphp.fr (T.X. Haen).

et al., 2014; Sarrafian et al., 2010; Shapiro et al., 2015). There is a need for a non-invasive tool, easy to use in clinical practice, and for research activities.

Shear Waves Elastography (SWE) provides a quantitative evaluation of biomechanical properties of soft tissues, as it measures the shear waves speed, which is related to tissue elasticity (Brum et al., 2014; Gennisson et al., 2003).

Although tendon tissue is anisotropic, a "transverse isotropic" model can be applied (Aubry et al., 2013; Brum et al., 2014; Gennisson et al., 2003). Indeed, the tendon consists of a parallel arrangement of fibers, with an axis of symmetry along the fibers corresponding to a hexagonal system (transverse isotropy) according to the viscoelasticity theory (Aubry et al., 2013; Zimmer and Cost, 1970).

SWE is non-invasive (Fink et al., 2004), real-time (Franchi-Abella et al., 2013), already available and easy to use (Zhang and Fu, 2013). It is currently used in various fields of medicine: diagnosis of liver diseases (Bavu et al., 2011), detection of cancerous (stiffer) tissues (Manickam et al., 2014)) for biopsy, especially for breast cancers (Han et al., 2012). Applications are being developed in the musculoskeletal field. For instance, Aubry et al. (2015) demonstrated that tendinopathy of AT was associated with significantly lower shear modulus, and Chen et al. (2013) demonstrated that shear modulus significantly decreased when AT was ruptured. Its reproducibility was studied for human cadaveric AT (Haen et al., 2015) (see below). SWE has been validated in animal tendon (Zhang and Fu, 2013) and animal muscle (Eby et al., 2013), showing significant correlation between elastographic measurements and tensile tests. But, to our knowledge, no correlation has been done between shear moduli obtained by SWE and mechanical properties from tensile tests in human tendon.

The aim of our project was to study whether the shear moduli of human AT, given by SWE, were correlated with the apparent elastic moduli of those tendons given by tensile tests, in order to validate the capacity of SWE to assess the biomechanical properties of human tendon.

2. Materials and methods

2. 1.Specimens

Human cadavers, from people having given their body to science, were studied, in collaboration with an Institute of Anatomy.[1]

Fourteen lower-limbs were obtained from 8 human cadavers (mean age at death: 87.9 ± 5.3 years old, range: 79–97; 10 women and 4 men), without signs of surgery history in lower limb. The time between death and dissection was about 2 months.

The cadavers were stored at 4 °C before harvesting of lower limbs. The limbs were then frozen at −20 °C. The limbs included the femur (with gastrocnemius insertions), the leg, and the foot (with AT insertion).

For the tests, the specimens were brought to room temperature of 20 °C for 18 h. They were hydrated by physiologic saline solution throughout all the preparation and test procedures.

2. 2.SWE in clinical-like conditions

First, the lower-limb laid prone on the examination table, with the knee extended. The ankle position was standardized by means of custom-made splints, controlled by goniometer. For each AT the ankle was positioned in three successive positions with a random sequence: The three positions #1, #2 and #3 respectively referred to 25° plantar flexion, neutral position and maximal dorsal flexion (Fig. 1).

SWE measurements were done blindly by a previously-trained operator, with the Aixplorer® system (V6.2, Supersonic Imagine, Aix-en-Provence, France). The following parameters were selected for SWE acquisitions: "Tendon" mode (in order to detect higher shear moduli), "Penetration" (in order to direct the shear waves towards the depth of the tendon), "High Definition", "Contrast"=80%. The region of interest (ROI) was set manually in a first step, ensuring that the whole tendinous area was included. The ultrasound probe was held manually, and applied with light pressure, on top of a generous amount of coupling gel, perpendicularly to the skin. The probe's orientation was sagittal, parallel to tendon fibers (controlled by ultrasounds mode), in order to meet the "transverse isotropy" criteria. SWE was performed randomly at three successive levels (respectively located at 0, 3 and 6 cm from the calcaneal insertion: Fig. 2).

The probe was kept motionless during the acquisition of a 10 s-movie of raw data. Data were stored in order to allow a blind off-line analysis. That analysis consisted in positioning a rectangular ROI in the tendon's area, for each picture of the 10 s-movie, very precisely thanks to a research-dedicated software (Vergari et al., 2014) (Fig. 3).

The ROI was set in order to be the largest as possible, but also excluding the fascia (risk of boundary effect (Brandenburg et al., 2014)). Hence, the ROI's size was not constant. The mean shear moduli μ_{SWE_Clin} of the ROI were automatically computed by the software, using the relation: $\mu_{SWE\_Clin}=\rho*c^2$ (Ates et al., 2015; Gennisson et al., 2003) where ρ is the density of the area (~1000 kg/m^3) and c is the shear waves speed, measured by the Aixplorer® system.

A previous study (Haen et al., 2015) has shown that the reproducibility of those measurements was equal to 33.4%, 22.1% and 20.7% for positions #1, 2 (neutral) and 3. It was considered satisfactory, but dependant to stretching-effect.

As a conclusion, for each AT, the following values were obtained (Table 1).

In order to study the influence of age on tendon elasticity, the mean μ_{SWE_Clin} were compared with the age at death.

2. 3.Tests with harvested AT

The limbs were then surgically prepared: the soft tissues were excised, in order to sample the AT with the triceps surae. All bone insertions, femoral and tibial triceps insertions as well as calcaneal AT insertions, were kept intact. The knee was locked in extension by means of external fixation. The tibia and fibula were sectioned. Each specimen was mounted on a testing machine (INSTRON ® 5566 High Wycombe, England, sensor: 10 kN, class 1, 4% precision in the range 0–100 N). The muscle-tendon complex was aligned, under gravity, with the axis of the load tensor. Fixation was made by means of cementation and metallic fixation of the bone extremities (Fig. 4). A 10 N pre-load was applied.

The geometrical parameters were obtained by direct measurements. The initial cross-sectional area (CSA) of the AT was calculated. It was assimilated as an ellipse, whose area was computed from the major and minor axis, measured by B-mode ultrasonography on transversal slices.

The SWE probe was positioned longitudinally (parallel to tendon body) at the distal part of the AT, corresponding to level 1 (Fig. 2). The probe was held by an articulated arm, including a spring, in order to keep a constant minimal pressure on the AT during the tensile test.

The specimen was first preconditioned for ten cycles, at 0.5 mm/s, with displacement between 2.5 and 7.5 mm in order to warm it. The anatomical preparation was subjected to tensile tests, at 3 different speeds (0.5, 1 and 2 mm/s) randomly, until 20 mm of elongation. SWE of the AT was performed simultaneously, with SWE acquisitions made every second. The load was measured by a load cell throughout the testing procedure and the global displacement of the musculotendinous complex was recorded by the testing machine. The displacement of the AT was measured by means of image correlation, thanks to an ultra-fast HD camcorder (Photron SA3, Photron USA, USA - San Diego, 1024*1024 resolution, acquisition frequency: 50 Hz), and a speckle pattern applied on the tendon (Fig. 5).

[1] Institut d'Anatomie UFR Biomédicale des Saints-Pères, Université René Descartes, 45 rue des Saints-Pères F-75270 Paris Cedex 06 (France).

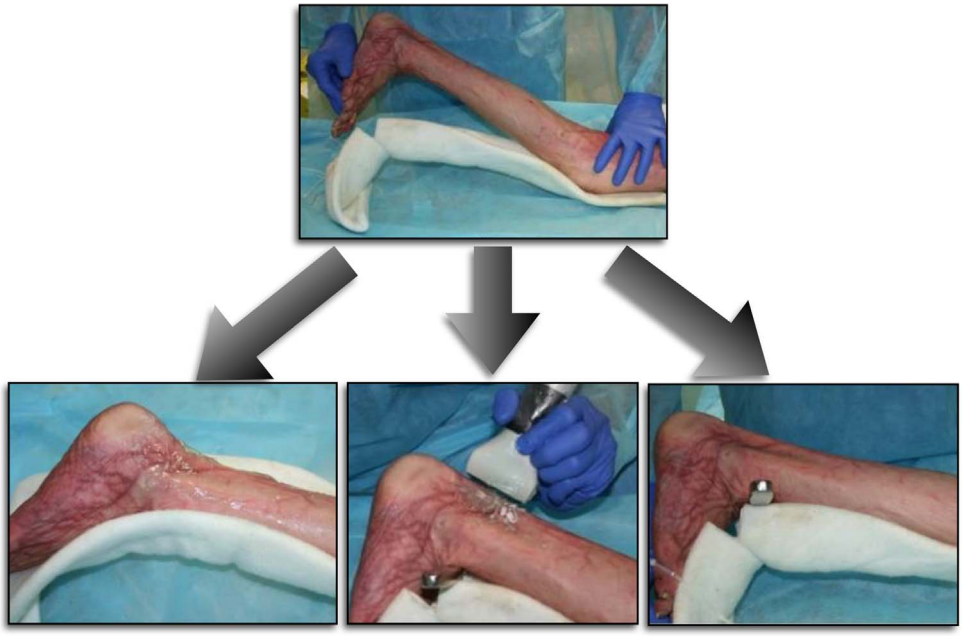

Fig. 1. Three ankle positions for SWE in clinical-like position: #1=25 ° plantar flexion, #2=neutral position and #3=maximal dorsal flexion.

Fig. 2. Three levels 1, 2 and 3 (at 0, 3 and 6 cm from tendon's bone insertion) for probe's position on the Achilles tendon.

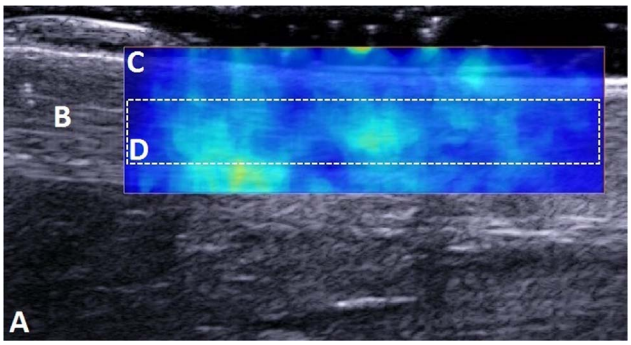

Fig. 3. Off-line analysis: Ultrasound echography (A), Shear Waves Elastography acquisition area (C), in which the region of interest (D) is placed (using homemade software), in order to correspond to the tendon's area (B).

SWE measurements were recorded and a blind off-line data analysis was done, which consisted in positioning the ROI in the tendon area, as previously described. The average shear moduli μ_{SWE_Exp} of the tendon's ROI were obtained.

Table 1
Main data collected with elastography in clinical-like conditions.

	Position 1	Position 2 (neutral)	Position 3
Level 1	$\mu_{SWE\_Clin\ pos1\ L1}$	$\mu_{SWE\_Clin\ pos2\ L1}$	$\mu_{SWE\_Clin\ pos3\ L1}$
Level 2	$\mu_{SWE\_Clin\ pos1\ L2}$	$\mu_{SWE\_Clin\ pos2\ L2}$	$\mu_{SWE\_Clin\ pos3\ L2}$
Level 3	$\mu_{SWE\_Clin\ pos1\ L3}$	$\mu_{SWE\_Clin\ pos2\ L3}$	$\mu_{SWE\_Clin\ pos3\ L3}$

2. 4Data analysis

The first SWE measurement, made at a level corresponding to level 1 just before the beginning of each tensile test (with the 10 N pre-load only), was registered separately. Those values were compared with mean shear moduli μ_{SWE_Clin} obtained by SWE in clinical-like conditions, for the same AT.

From the collected tensile test data, the engineering stress (σ) was calculated by dividing the force by the measured cross-sectional area, while the strain (ε) was obtained by image correlation (Fig. 5). Image correlation is a technique which consists in analyzing every pictures of AT registered by the HD camcorder, thanks to the specific in-house Matlab software. Vertical lines were numerically traced over the dots of the speckle pattern. Then, during tendon's elongation, the strain of every line was measured. The mean strain of every lines corresponded to the mean strain of the AT's surface.

The stress/strain curve was plotted. The apparent elastic modulus E_{app_Exp} was obtained by calculating the derivative of each point of the stress/strain curve.

The curves representing the apparent elastic moduli E_{app_Exp} (from tensile test) and shear moduli μ_{SWE_Exp} (from SWE), versus strain, were plotted. The correlation between E_{app_Exp} and μ_{SWE_Exp} was studied, by calculating the deviation between the 2 curves.

A two-way ANOVA was used to evaluate the effects of the specimens' geometrical parameters on the shear modulus. Post-hoc Tukey comparisons were used as follow-up to the significant ANOVA results. Significance was set at $p < 0.05$ for all statistical comparisons.

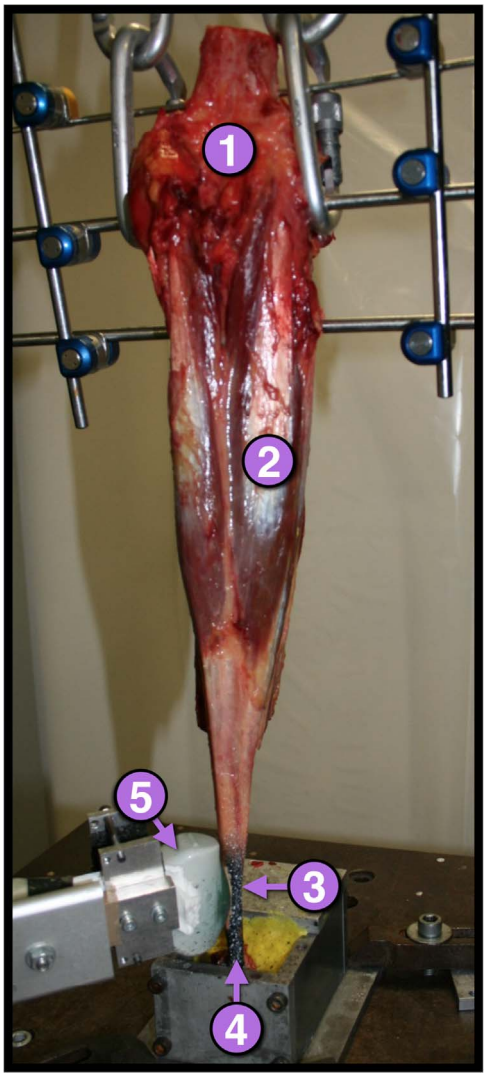

Fig. 4. Experimental set-up: anatomical specimen mounted in the material testing machine. 1. Knee, 2. Triceps surae, 3. Achilles tendon, 4. Calcaneus cemented in a bucket fixed on the testing machine, 5. Elastographic probe held by an articulated arm.

3. Results

3. 1SWE in clinical-like conditions

SWE made in clinical conditions demonstrated an increase of shear moduli with AT's strain, as the values increased from position #1 (25° plantar flexion) to position #3 (maximal dorsal flexion, which corresponded to an average 7.9 ± 7.4° (range: 0–20°) of dorsal flexion), see boxplots (Fig. 6).

Shear moduli, in clinical-like conditions (in neutral position) and on harvested tendon, decreased with increasing specimen's age at death ($p < 0.05$).

3. 2Comparison between SWE of entire limb (clinical-like conditions) and on harvested tendon

Average shear moduli of harvested AT μ_{SWE_init}, given by SWE made at 10 N pre-load before the tensile tests, were significantly correlated with μ_{SWE_Clin}, the shear moduli of the same AT made at level 1, previously in clinical-like condition ($p < 0.05$), in ankle position #2 (neutral position) only.

3. 3Comparison between SWE and tensile tests

Three specimens were inoperable: for 2 specimens the speckle pattern was unusable, and for one specimen the probe moved away from the AT, causing an aberrant shear modulus curve. The final analysis was done on 11 specimens.

The correlation between the 2 curves (representing E_{app_Exp} and μ_{SWE_Exp} versus strain) changed, for every specimen, after a «disruption point» (see Fig. 7). That point was computed for every specimen. It occurred at mean 0.161 ± 0.11% strain.

The correlation coefficient R^2, between E_{app_Exp} and μ_{SWE_Exp}, was equal to 0.95 ± 0.05 for the region before the disruption point. This correlation was statistically significant ($p < 0.05$). There was no correlation after that point.

During the tests on the testing machine, there was no tendon rupture, because the higher strain occurred in the muscular part of the musculotendinous complex: the maximal strain in the tendon was equal to 0.3% in average, while it was equal to 6% for the entire musculotendinous complex.

4. Discussion

We demonstrated a significant correlation between SWE of AT performed in clinical-like conditions (in neutral position) and SWE performed in harvested tendon. We also found a significant correlation between SWE performed on harvested tendon and apparent elastic moduli obtained with tensile tests (for 11 specimens). As a consequence, we can suppose that SWE of AT in clinical-like conditions is related to tensile tests. To our knowledge, such findings have never been reported in human tendon. So far, the ability of SWE to reliably assess biomechanical properties of a tendon (Yeh et al., 2016; Zhang and Fu, 2013) or muscle (Eby et al., 2013) was only demonstrated in animal models.

We also confirmed that shear moduli increased with AT's strain, as demonstrated by Aubry et al. (2013). We have studied the relation between age and SWE. The shear moduli decreased for aged specimens, as previously demonstrated (Aubry et al., 2013; Ruan et al., 2015). It can be explained by the replacement of type I collagen fibers by type III in degenerative tendons, as well as pathological tendons, which are less elastic and more prone to rupture (Ruan et al., 2015).

Wang has described the mechanobiology of the tendon (Wang, 2006): before 2% strain, the tendon's comportment corresponds to the “toe-region”, which is just before the “linear region”, both being in physiologic range (Maganaris et al., 2008). In our study, the AT's maximal strain was equal to 0.3% in average. Then, the stress/strain curve can only offer an approximation of the elastic modulus, but corresponds to physiologic range. We had chosen to keep the muscular part of the tendinomuscular complex, for tensile test, in order to be as close as possible to physiological conditions. Indeed, others studies have proposed to test the tendons only, but the fixation technique (among others, with clamps…) raises specific problems (Maganaris et al., 2008). Due to the much bigger elasticity of muscle compared with tendon, leading to early muscle breakage, it seems difficult to obtain a higher strain for tendon with this technique.

All findings were obtained in spite of a technically challenging protocol. This protocol explained the failure for the correlation to biomechanical test study for three specimens, and probably the lower correlation for highest strain (in particular after the «disruption point»). For example, the experimental set up included many interfaces, by which forces may have been taken up, and this phenomenon may vary among specimens (Zhang and Fu, 2013).

Keeping the probe with a light pressure on the tendon, during the tensile test, was a main concern (Kot et al., 2012). That's why we used an articulated arm with a spring, as well as a large amount of gel between the probe and the AT.

We also excluded saturated areas (corresponding to hyper-pressure), when positioning the ROI during data analysis (Dewall et al.,

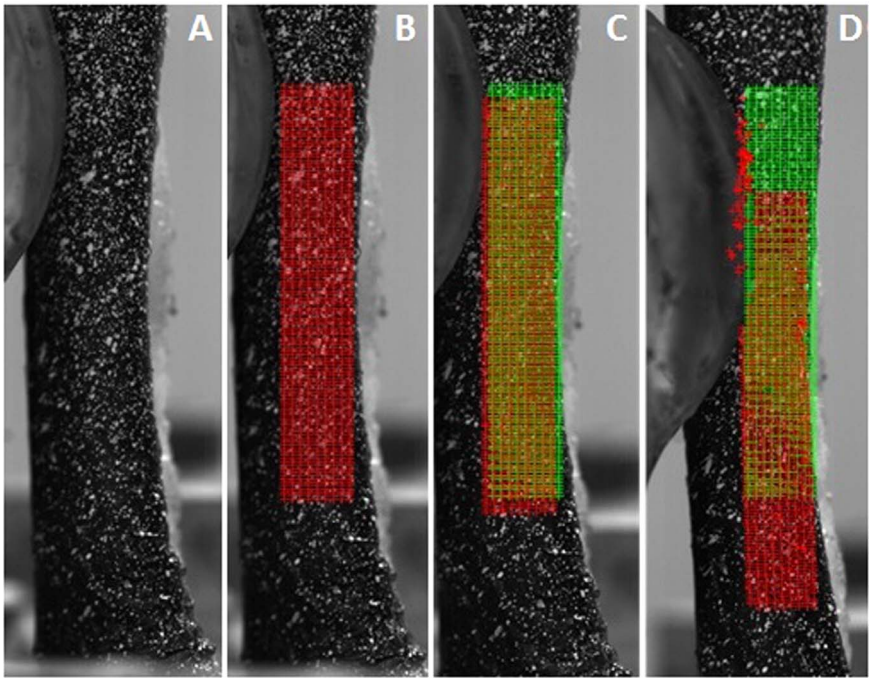

Fig. 5. Tendon's displacement measured by means of image correlation: Speckle pattern on the Achilles Tendon (A), with mesh corresponding to different points. The red mesh corresponds to the initial configuration (B), the green one represents the displacement.

2014). The articulated arm also allowed keeping the probe parallel to tendon fibers, which is a major concern in order to maintain "transverse isotropy" conditions (Aubry et al., 2013), and given that only a 10° change in probe's orientation can lead up to a 30% increase in error (Gennisson et al., 2003). Collagen fibers in AT have a helicoidal arrangement (Aubry et al., 2015), which could make it difficult to keep the parallelism. Posteriori controls with screenshots of B-mode ultrasonographic pictures showed a good orientation.

Nevertheless, the articulated arm seems to have failed to prevent error with highest strain, explaining the absence of correlation after the disruption point.

We intentionally avoid the use of an articulated arm (unlike Koo et al. (2014)) nor a specific "gel pad", for the "clinical-like" study, in order to be as close as possible to clinical conditions.

We set the SWE's technical settings as recommended by the manufacturer, and confirmed by Kot et al. (2012). The acquisition time was equal to 8–12 s (Kot et al., 2012), hereafter the risk of error, due to probe's displacement, increases. We also used a ROI corresponding to the size of the anatomical structure which was studied, as recommended by Kot et al. (2012). The limits of the ROI precisely fitted the anatomical limits of the AT in order to maximize the size of tissue analyzed, thereby reducing the risk of error (Ates et al., 2015; Kot et al., 2012). Moreover, we thoroughly avoided to include the hyper-echogenic borders because of the risk of boundary effect (Brandenburg et al., 2014). The use of a research-dedicated software allowed precise positioning of the ROI, and blind realization of the SWE, which was distinct from data collection.

The AT's displacement was measured by means of image correlation, which detects displacements lower than 1 mm. It needs a quality speckle pattern, but also a clear picture, yet focus can be lost if tendon

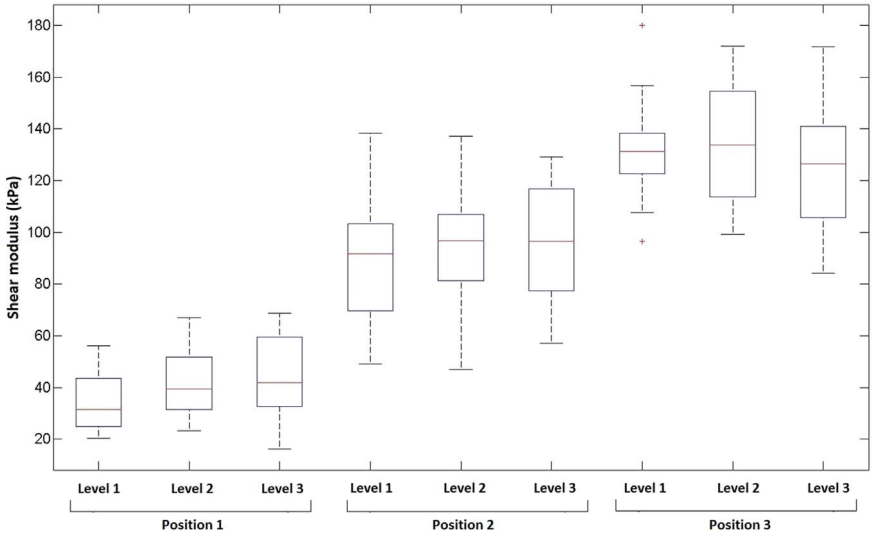

Fig. 6. Boxplots of shear moduli, depending on position (positions #1, #2 and #3 respectively for 25° plantar flexion, neutral position and maximal dorsal flexion) and level of measure, in clinical-like conditions.

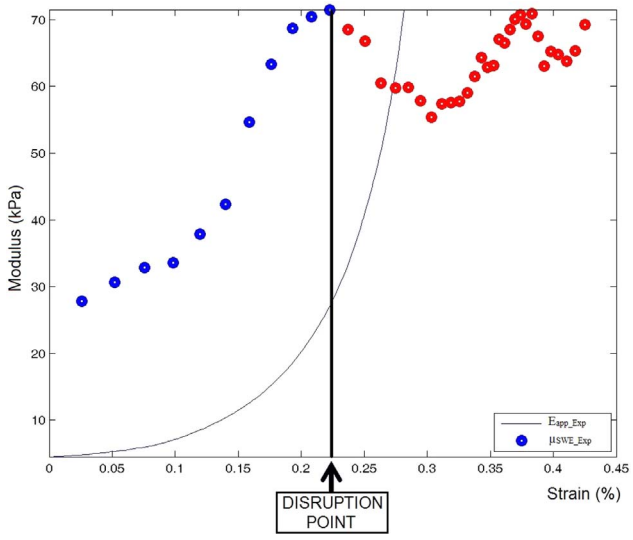

Fig. 7. Curves representing E_{app_Exp} (continuous curve) and μ_{SWE_Exp} (dotted curve) versus strain, for a typical specimen.

moves with the strain. This explains the failure for two specimens, whose speckle pattern was unusable.

Moreover, the image correlation measured the AT's displacement superficially, whereas SWE was performed also in depth. Yet it is possible that the different layers moved differently from superficial part to depth (Bilston and Tan, 2015), especially with stiffening effect of the painting applied on the AT. Similarly, soft tissues around the AT can have mechanical action (Zhang and Fu, 2013). That's why all the soft tissues around the tendon (including the perimysium) were removed, while making sure not to have weakened it.

Some authors have stated that SWE of AT was not reliable, as the shear moduli may exceed the upper detection limit (Cortes et al., 2015; Dewall et al., 2014), currently equal to 800 kPa (Aubry et al., 2013). But we did not reach those values (Fig. 6). And we did not observe any saturation effect, unlike Dewall et al. (2014), which consisted in a low increase of shear moduli, between neutral and dorsiflexion. In fact, our mean values, concerning cadaveric ATs, were lower than generally published values of AT's shear moduli in clinical studies (Aubry et al., 2013; Chen et al., 2013). Indeed, our study was performed in vitro, with fresh-frozen cadaveric tendons. The specimens were fresh-frozen but, according to Clavert et al. (2001), it induces minimal modification of mechanical properties, the stress-strain curve's aspect being similar. Using cadaveric tendons, the conditions were not physiological (concerning tissue temperature, perfusion, hydration… (Gras et al., 2012)), although we standardized the room temperature, and made sure to provide regular hydration with saline solution throughout all the procedure. We also respected the original morphology. All bone insertions were preserved, for optimal fixation in the testing machine (unlike fixation with a clamp, which might induce a slip of the tendon). The original orientation of anatomic elements was respected, in order forces apply in the physiological direction during the effort.

Recent publications have also stated that, for the tendons, the shear wave lengths are larger than the tendon thickness, resulting in a guided propagation of waves (Aubry et al., 2015; Brum et al., 2014). Then, the shear wave speed must be assessed as a function of frequency, in order to obtain the real shear modulus (shear "dispersion analysis" (Brum et al., 2014; Helfenstein-Didier et al., 2016)). Although such a function is not available in clinical practice, it could explain poor correlation at higher strain. Moreover, it has been shown that correlation between conventional SWE and modulus measured using the shear wave dispersion technique was worse at higher strain (Helfenstein-Didier et al., 2016). At last, at high deformation, strain and stress are no more negligible, and the shear wave propagation is modified due to the inner stress of the tendon ("acoustoelasticity theory"). Shear nonlinear parameters intervene and, although they are not easily measurable, they should be taken into account (Renier et al., 2007).

Helfenstein-Didier et al. (2016), in their recent comparison of conventional SWE and new dispersion technique, found a high significant correlation (r=0.84). The authors concluded that conventional SWE remains relevant for tendon characterization, in clinical studies.

5. Conclusion

We have evaluated SWE of human cadaveric AT. The SWE of AT, in clinical-like conditions, was correlated with SWE of the same tendons once harvested. And the latter measurements were correlated with stress/strain curves given by tensile tests of the same tendons. Therefore, being correlated to its stress-strain curve, SWE can provide biomechanical information of the human AT.

The present study strongly suggests that SWE performed at bedside may be a reliable tool for assessing in-vivo and non-invasively the biomechanical properties of the AT. Further clinical studies are now required to validate this hypothesis.

Disclosure of interest

The authors declare that they have no conflicts of interest concerning this article.

Acknowledgement

The authors are grateful to the ParisTech BiomecAM Chair program for funding.

The authors also thank Professor O. Gagey for his support during this study, and Claudio Vergari for his decisive help.

References

Ates, F., Hug, F., Bouillard, K., Jubeau, M., Frappart, T., Couade, M., Bercoff, J., Nordez, A., 2015. Muscle shear elastic modulus is linearly related to muscle torque over the entire range of isometric contraction intensity. J. Electromyogr. Kinesiol. 25, 703–708. http://dx.doi.org/10.1016/j.jelekin.2015.02.005.

Aubry, S., Nueffer, J.-P.P., Tanter, M., Becce, F., Vidal, C., Michel, F., 2015. Viscoelasticity in Achilles Tendonopathy: quantitative assessment by using real-time shear-wave elastography. Radiology 274, 821–829. http://dx.doi.org/10.1148/radiol.14140434.

Aubry, S., Risson, J.-R., Kastler, A., Barbier-Brion, B., Siliman, G., Runge, M., Kastler, B., 2013. Biomechanical properties of the calcaneal tendon in vivo assessed by transient shear wave elastography. Skelet. Radiol. 42, 1143–1150. http://dx.doi.org/10.1007/s00256-013-1649-9.

Bavu, É., Gennisson, J.-L., Couade, M., Bercoff, J., Mallet, V., Fink, M., Badel, A., Vallet-Pichard, A., Nalpas, B., Tanter, M., Pol, S., 2011. Noninvasive in vivo liver fibrosis evaluation using supersonic shear imaging: a clinical study on 113 Hepatitis C virus patients. Ultrasound Med. Biol. 37, 1361–1373. http://dx.doi.org/10.1016/j.ultrasmedbio.2011.05.016.

Bilston, L.E., Tan, K., 2015. Measurement of passive skeletal muscle mechanical properties in vivo: recent progress, clinical applications, and remaining challenges. Ann. Biomed. Eng. 43, 261–273. http://dx.doi.org/10.1007/s10439-014-1186-2.

Brandenburg, J.E., Eby, S.F., Song, P., Zhao, H., Brault, J.S., Chen, S., An, K., 2014. Ultrasound elastography: the new frontier in direct measurement of muscle stiffness. Arch. Phys. Med. Rehabil. 95, 2207–2219. http://dx.doi.org/10.1016/j.apmr.2014.07.007.

Brum, J., Bernal, M., Gennisson, J.L., Tanter, M., 2014. In vivo evaluation of the elastic anisotropy of the human Achilles tendon using shear wave dispersion analysis. Phys. Med. Biol. 59, 505–523. http://dx.doi.org/10.1088/0031-9155/59/3/505.

Bruns, J., Kampen, J., Kahrs, J., Plitz, W., 2014. Achilles tendon rupture: experimental results on spontaneous repair in a sheep-model. Knee Surgery. Sport. Traumatol. Arthrosc. 8, 364–369. http://dx.doi.org/10.1007/s001670000149.

Chen, X.-M., Cui, L.-G., He, P., Shen, W.-W., Qian, Y.-J., Wang, J.-R., 2013. Shear wave elastographic characterization of normal and torn Achilles tendons: a pilot study. J. Ultrasound Med. 32, 449–455.

Clavert, P., Kempf, J.F., Bonnomet, F., Boutemy, P., Marcelin, L., Kahn, J.L., 2001. Effects of freezing/thawing on the biomechanical properties of human tendons. Surg. Radiol. Anat. 23, 259–262.

Cortes, D.H., Suydam, S.M., Silbernagel, K.G., Buchanan, T.S., Elliott, D.M., 2015. Continuous shear wave elastography: a new method to measure viscoelastic properties of Tendons in vivo. Ultrasound Med. Biol. 41, 1518–1529. http://dx.doi.org/10.1016/j.ultrasmedbio.2015.02.001.

Dewall, R.J., Slane, L.C., Lee, K.S., Thelen, D.G., 2014. Spatial variations in Achilles tendon shear wave speed. J. Biomech. 47, 2685–2692. http://dx.doi.org/10.1016/j.jbiomech.2014.05.008.

Eby, S.F., Song, P., Chen, S., Chen, Q., Greenleaf, J.F., An, K.-N., 2013. Validation of shear wave elastography in skeletal muscle. J. Biomech. 46, 2381–2387. http://dx.doi.org/10.1016/j.jbiomech.2013.07.033.

Fink, M., Bercoff, Tanter, 2004. Supersonic shear imaging: a new technique for soft tissue elasticity mapping. IEEE Trans. Ultrason. Ferroelectr. Freq. Control 51, 396–409.

Franchi-Abella, S., Elie, C., Correas, J.-M., 2013. Ultrasound elastography: advantages, limitations and artefacts of the different techniques from a study on a phantom. Diagn. Interv. Imaging 94, 497–501. http://dx.doi.org/10.1016/j.diii.2013.01.024.

Gennisson, J.-L., Catheline, S., Chaffaï, S., Fink, M., 2003. Transient elastography in anisotropic medium: application to the measurement of slow and fast shear wave speeds in muscles. J. Acoust. Soc. Am. 114, 536. http://dx.doi.org/10.1121/1.1579008.

Gras, L.-L., Mitton, D., Viot, P., Laporte, S., 2012. Hyper-elastic properties of the human sternocleidomastoideus muscle in tension. J. Mech. Behav. Biomed. Mater. 15, 131–140. http://dx.doi.org/10.1016/j.jmbbm.2012.06.013.

Haen, T.X., Roux, A., Labruyere, C., Vergari, C., Rouch, P., Gagey, O., Soubeyrand, M., Laporte, S., 2015. Shear wear elastography of the human Achilles tendon: a cadaveric study of factors influencing the repeatability. Comput. Methods Biomech. Biomed. Eng. 18, 1954–1955. http://dx.doi.org/10.1080/10255842.2015.1069578.

Han, Y., Kim, D.W., Kwon, H.J., 2012. Application of digital image cross-correlation and smoothing function to the diagnosis of breast cancer. J. Mech. Behav. Biomed. Mater. 14, 7–18. http://dx.doi.org/10.1016/j.jmbbm.2012.05.007.

Helfenstein-Didier, C., Andrade, R.J., Brum, J., Hug, F., Tanter, M., Nordez, A., Gennisson, J.-L., 2016. In vivo quantification of the shear modulus of the human Achilles tendon during passive loading using shear wave dispersion analysis. Phys. Med. Biol. 61, 2485–2496. http://dx.doi.org/10.1088/0031-9155/61/6/2485.

Hess, G.W., 2010. Achilles tendon rupture: a review of etiology, population, anatomy, risk factors, and injury prevention. Foot Ankle Spec. 3, 29–32. http://dx.doi.org/10.1177/1938640009355191.

Józsa, L., Kvist, M., Bálint, B.J., Reffy, A., Järvinen, M., Lehto, M., Barzo, M., 1989. The role of recreational sport activity in Achilles tendon rupture. A clinical, pathoanatomical, and sociological study of 292 cases. Am. J. Sport. Med. 17, 338–343.

Koo, T.K., Guo, J.-Y., Cohen, J.H., Parker, K.J., 2014. Quantifying the passive stretching response of human tibialis anterior muscle using shear wave elastography. Clin. Biomech. 29, 33–39. http://dx.doi.org/10.1016/j.clinbiomech.2013.11.009.

Kot, B.C.W., Zhang, Z.J., Lee, A.W.C., Leung, V.Y.F., Fu, S.N., 2012. Elastic modulus of muscle and tendon with shear wave ultrasound elastography: variations with different technical settings. PLoS One 7, e44348. http://dx.doi.org/10.1371/journal.pone.0044348.

Lantto, I., Heikkinen, J., Flinkkilä, T., Ohtonen, P., Leppilahti, J., 2014. Epidemiology of Achilles tendon ruptures: increasing incidence over a 33-year period. Scand. J. Med. Sci. Sport., 1–6. http://dx.doi.org/10.1111/sms.12253.

Maganaris, C.N., Narici, M.V., Maffulli, N., 2008. Biomechanics of the Achilles tendon. Disabil. Rehabil. 30, 1542–1547. http://dx.doi.org/10.1080/09638280701785494.

Manickam, K., Machireddy, R.R., Seshadri, S., 2014. Characterization of biomechanical properties of agar based tissue mimicking phantoms for ultrasound stiffness imaging techniques. J. Mech. Behav. Biomed. Mater. 35, 132–143. http://dx.doi.org/10.1016/j.jmbbm.2014.03.017.

Marcos, R.L., Arnold, G., Magnenet, V., Rahouadj, R., Magdalou, J., Lopes-Martins, R.Á.B., 2014. Biomechanical and biochemical protective effect of low-level laser therapy for Achilles tendinitis. J. Mech. Behav. Biomed. Mater. 29, 272–285. http://dx.doi.org/10.1016/j.jmbbm.2013.08.028.

Renier, M., Gennisson, J.-L., Tanter, M., Catheline, S., Barriere, C., Royer, D., Fink, M., 2007. 7B-2 Nonlinear Shear Elastic Moduli in Quasi-Incompressible Soft Solids. In: Proceedings of the 2007 IEEE Ultrasonics Symposium. pp. 554–557. doi:10.1109/ULTSYM.2007.144

Ruan, Z., Zhao, B., Qi, H., Zhang, Y., Zhang, F., Wu, M., Shao, G., 2015. Elasticity of healthy Achilles tendon decreases with the increase of age as determined by acoustic radiation force impulse imaging. Int. J Clin. Exp. Med. 8, 1043–1050.

Sarrafian, T.L., Wang, H., Hackett, E.S., Yao, J.Q., Shih, M.-S., Ramsay, H.L., Turner, A.S., 2010. Comparison of Achilles tendon repair techniques in a sheep model using a cross-linked Acellular porcine dermal patch and platelet-rich plasma fibrin matrix for augmentation. J. Foot Ankle Surg. 49, 128–134. http://dx.doi.org/10.1053/j.jfas.2009.12.005.

Shapiro, E., Grande, D., Drakos, M., 2015. Biologics in Achilles tendon healing and repair: a review. Curr. Rev. Musculoskelet. Med. 8, 9–17. http://dx.doi.org/10.1007/s12178-015-9257-z.

Vergari, C., Rouch, P., Dubois, G., Bonneau, D., Dubousset, J., Tanter, M., Gennisson, J.-L., Skalli, W., 2014. Non-invasive biomechanical characterization of intervertebral discs by shear wave ultrasound elastography: a feasibility study. Eur. Radiol. 24, 3210–3216. http://dx.doi.org/10.1007/s00330-014-3382-8.

Wang, J.H.-C., 2006. Mechanobiology of tendon. J. Biomech. 39, 1563–1582. http://dx.doi.org/10.1016/j.jbiomech.2005.05.011.

Yeh, C.L., Kuo, P.L., Gennisson, J.L., Brum, J., Tanter, M., Li, P.C., 2016. Shear wave measurements for evaluation of tendon diseases. IEEE Trans. Ultrason. Ferroelectr. Freq. Control 63, 1906–1921. http://dx.doi.org/10.1109/TUFFC.2016.2591963.

Zhang, Z.J., Fu, S.N., 2013. Shear elastic modulus on patellar tendon captured from supersonic shear imaging: correlation with tangent traction modulus computed from material testing system and test – retest reliability. PLoS One 8, 1–9. http://dx.doi.org/10.1371/journal.pone.0068216.

Zimmer, J.E., Cost, J.R., 1970. Determination of the elastic constants of a unidirectional fiber composite using ultrasonic velocity measurements. J. Acoust. Soc. Am. 47, 795–803. http://dx.doi.org/10.1121/1.1911962.